Journal of King Saud University – Science (2015) 27, 15–22

King Saud University

Journal of King Saud University – Science

www.ksu.edu.sa

www.sciencedirect.com

ORIGINAL ARTICLE

# Gainful utilization of the highly intransigent weed ipomoea in the synthesis of gold nanoparticles

**Tasneem Abbasi** *, **J. Anuradha, S.U. Ganaie, S.A. Abbasi**

*Centre for Pollution Control and Environmental Engineering, Pondicherry University, 605 014, Puducherry*

Received 15 October 2013; accepted 11 April 2014
Available online 30 April 2014

**KEYWORDS**

*Ipomoea carnea*;
*I. fistulosa*;
Gold nanoparticles;
Biomimetic synthesis

**Abstract** The paper presents a new method for the biomimetic synthesis of gold nanoparticles (GNPs), in which a highly invasive and harmful weed *Ipomoea carnea* has been employed for the first time as the main bioagent. Extracts of all the three basic components of the plant – leaves, stem and root – were explored and were found to be suitable in effecting the GNP synthesis. The electron micrographs of the synthesized GNPs revealed the presence of particles of monodispersed spherical and polydispersed triangular, hexagonal, polygonal, rod, and truncated triangular shapes in sizes ranging 3–40 and 10–100 nm, respectively. The presence of gold atoms was confirmed from the EDAX and X-ray diffraction studies. The FT-IR spectral study indicated that the polysaccharides and proteins in the plant extract could have been responsible for the reduction of gold ions to GNPs and the latter's stabilization.



## 1. Introduction

As nanotechnology finds increasing application across diverse fields of human endeavor, there is a growing need to develop more and more clean and frugal procedures for the generation and assembly of nanoparticles. Among the very attractive options is the use of biomimetic methods which mimic the way in which nanoparticles are synthesized in nature under benign environmental conditions, with benign chemicals, and with minimum inputs of energy. Using extracts of different plants (botanical species) to extracellularly synthesize nanoparticles is one of the most promising biomimetic routes. Unlike other biomimetic options, which rely on microorganisms, plant-based option is generally simpler and quicker (Anuradha et al., 2010, 2011a,b; Abbasi et al., 2014).

Beginning with the pioneering work of Shankar et al. (2003), gold nanoparticles (GNPs) have been synthesized using a myriad of plant species (Abbasi et al., 2014). These include medicines such as neem and lemongrass (Shankar et al., 2004a,b), cosmetics such as clove (Singh et al., 2010), stimulants such as tea (Begum et al., 2009), nuts such as cashew (Sheny et al., 2011), ornamentals such as rose and dandelion (Dubey et al., 2010; Tettey et al., 2012), and a very large variety of species used as food or fodder (Dubey et al., 2013; Abbasi et al., 2014). But two aspects have limited the use of procedures based on these species. The first of these stems from

* Corresponding author. Concurrently Visiting Associate Professor, Worcester Polytechnic Institute, Worcester, MA 01609, USA.
E-mail addresses: tasneem.abbasi@gmail.com (T. Abbasi), abbasi.cpee@gmail.com (S.A. Abbasi).

Peer review under responsibility of King Saud University.

ELSEVIER Production and hosting by Elsevier

http://dx.doi.org/10.1016/j.jksus.2014.04.001

**Table 1** Wavelengths of absorption peaks ($\lambda_{max}$, nm) and corresponding absorbance of gold nanoparticle suspensions synthesized using extracts of ipomoea.

| Plant part used for preparing the extract | Metal: extract concentration ratio | Reaction duration (h) | | | | | | | | | |
|---|---|---|---|---|---|---|---|---|---|---|---|
| | | 2 | | 4 | | 6 | | 24 | | 48 | |
| | | $\lambda_{max}$ | Absorbance | $\lambda_{max}$ | Absorbance | $\lambda_{max}$ | Absorbance | $\lambda_{max}$ | Absorbance | $\lambda_{max}$ | Absorbance |
| Leaf (LE) | 1:3 | 538 | 1.03 | 538 | 2.20 | 539 | 2.56 | 537 | 2.97 | 536 | 2.94 |
| | 1:7 | 536 | 2.56 | 537 | 2.59 | 536 | 2.61 | 536 | 2.69 | 536 | 2.66 |
| | 1:15 | – | – | – | – | – | – | – | – | – | – |
| | 1:25 | – | – | – | – | – | – | – | – | – | – |
| | 1:60 | – | – | – | – | – | – | – | – | – | – |
| Stem (SE) | 1:3 | – | – | – | – | 560 | 0.29 | 565 | 1.35 | 559 | 0.70 |
| | 1:7 | – | – | 547 | 0.24 | 568 | 1.26 | 568 | 1.77 | 551 | 0.73 |
| | 1:15 | 539 | 1.93 | 539 | 2.34 | 538 | 2.56 | 532 | 2.68 | 536 | 2.55 |
| | | | | | | | | 846 | 0.99 | 846 | 1.01 |
| | 1:25 | 533 | 2.01 | 534 | 2.03 | 536 | 2.02 | 539 | 2.02 | 542 | 2.00 |
| | 1:60 | – | – | – | – | – | – | – | – | – | – |
| Root (RE) | 1:3 | – | – | – | – | 553 | 0.33 | 562 | 0.93 | 565 | 1.25 |
| | 1:7 | 554 | 0.57 | 553 | 1.09 | 553 | 1.46 | 554 | 1.46 | 548 | 1.79 |
| | 1:15 | 537 | 1.97 | 536 | 2.23 | 536 | 2.30 | 536 | 2.26 | 534 | 2.23 |
| | 1:25 | 533 | 1.98 | 533 | 1.98 | 533 | 2.01 | 532 | 1.93 | 533 | 1.93 |
| | | 833 | 1.22 | 833 | 1.23 | 832 | 1.22 | 832 | 1.14 | 832 | 1.13 |
| | 1:60 | – | – | – | – | – | – | – | – | – | – |

the fact that all these species already have designated uses and ready markets. Employing them for GNP synthesis would mean compromising with one or more of their other uses. The other drawback is that nearly all reported methods utilize either the leaves or the fruits of the given species, leaving the rest of the plant, especially the stem and the roots, unutilized.

The present work is made distinct by its two attributes. Firstly it is based on a plant which is freely available and has no competing use. Secondly it utilizes all the plant parts, leaving nothing to waste. Indeed the species on which the present work is based—ipomoea (*Ipomoea carnea*, also called *Ipomoea fistulosa*)—is a highly pernicious amphibian weed which

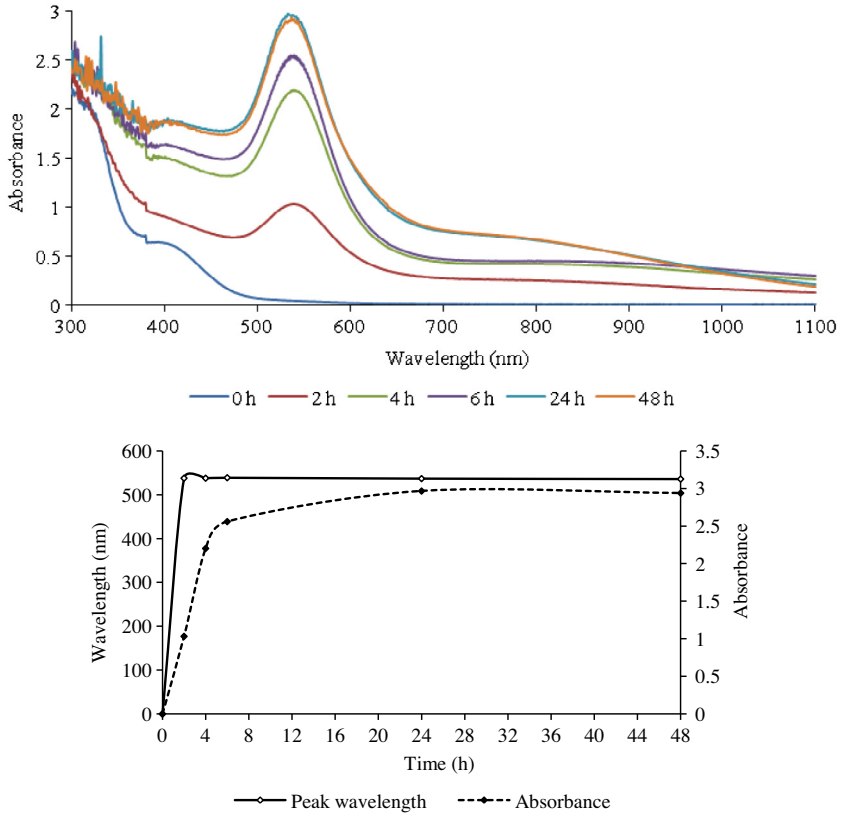


**Figure 1** The UV–Visible spectra of GNPs formed with gold (III) and the leaf extract of ipomoea (top), and the change in $\lambda_{max}$ as a function of time.

has been a scourge of land-masses and shallow water bodies all over the tropical regions of the world. In India alone, losses caused by ipomoea have been estimated to exceed several thousand crore rupees per annum (Chari et al., 2005; Abbasi et al., 2008). As of now there is no economically viable method with which large enough quantities of this weed can be utilized to exercise control over its proliferation. Nor is it possible to destroy this weed with chemical or biological means without seriously endangering the environment. The present method, besides providing a freely available bioagent for GNP synthesis, also creates an opportunity to harvest the bioagent in large quantities, thereby exerting some control over its negative environmental impacts.

## 2. Experimental

All chemicals were of analytical regent grade unless otherwise specified. Deionized water, double distilled in all-glass stills, was used throughout.

### *2.1. Preparation of aqueous extracts of the leaf, stem and root of ipomoea*

*I. carnea* was collected from its place of prevalence in the campus of the Pondicherry University. Fresh, mature, and disease-free plant portions were washed to clear off the attached soil, then dipped in saline water to sterilize their surface, and washed again before blotting them dry. Several randomly picked plant samples were weighed and then dried at 105 °C to a constant weight (APHA, 2012). On the basis of the dry weight thus obtained, extracts for nanoparticle synthesis were made by boiling 2 g dry weight equivalent of the plant material with 100 ml of water for 5 min. The contents were filtered through a Whatman number 42 filter paper and the filtrate was stored at 4 °C. Reconnoitery experiments indicated that the extracts retained their integrity for up to 3 days, as evidenced by the extent of intensity of nanoparticles generated by them. Hence in all the experiments the extracts were used within three days of preparation.

### *2.2. Au (III) solution*

A $10^{-3}$ M aqueous solution of Au (III) was prepared using $HAuCl_4$. The stock solution was stored in amber bottles covered with black sheets.

### *2.3. Nanoparticle synthesis*

Different metal-extract concentrations varying in ratios spanning 1:1–1:60 were explored to see their influence on the shapes and sizes of the GNPs that were formed. It was seen that the GNPs began forming almost immediately as indicated by the appearance of pinkish red or purple color which grew in intensity with time. The progress of the synthesis was tracked

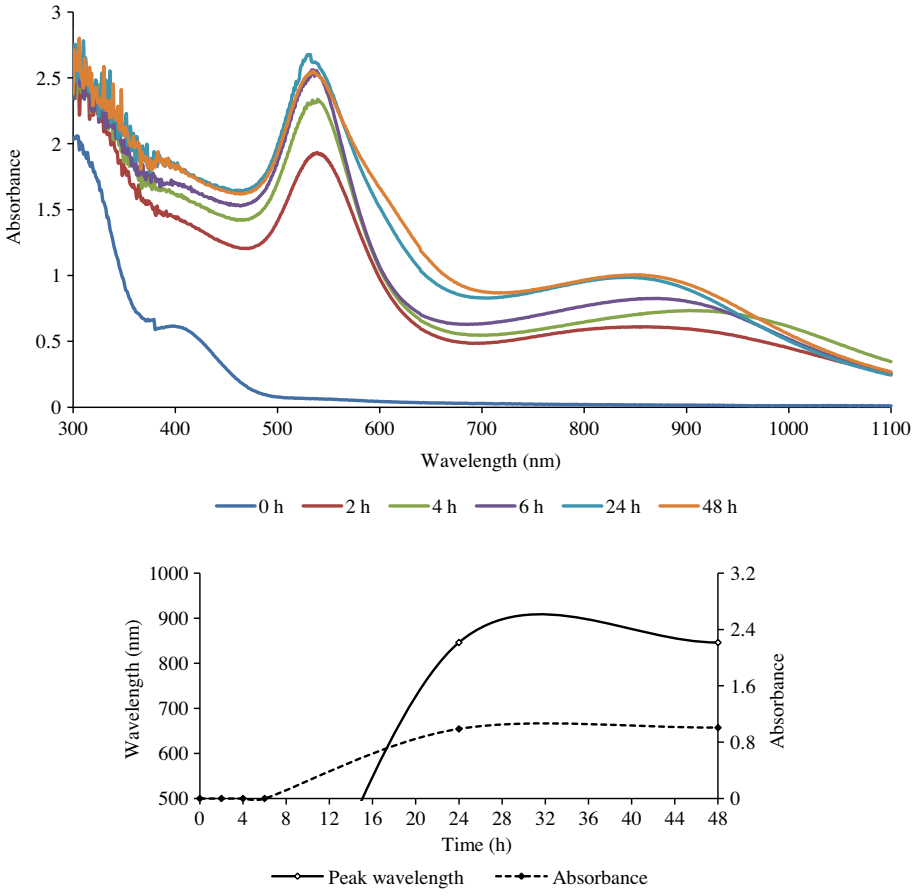


**Figure 2** The UV–Visible spectra of GNPs formed with gold (III) and the stem extract of ipomoea (top), and the change in $\lambda_{max}$ as a function of time.

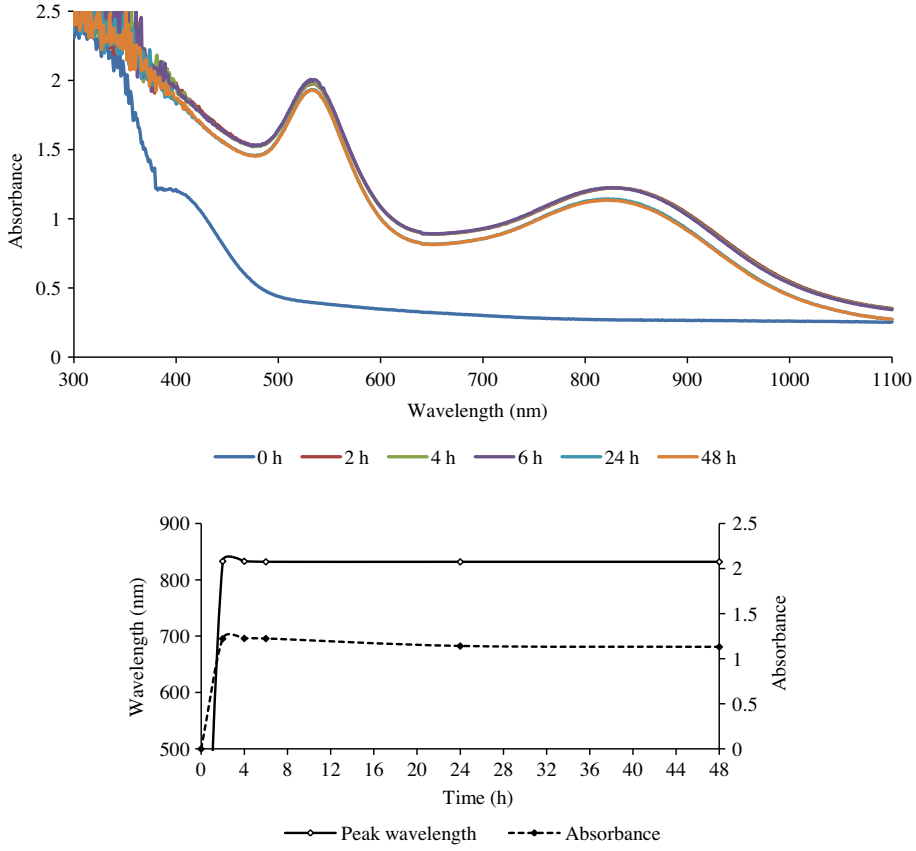


**Figure 3** The UV–Visible spectra of GNPs formed with gold (III) and the root extract of ipomoea (top), and the change in $\lambda_{max}$ as a function of time.

continuously by monitoring the UV–Visible spectrum of the metal-extract mixture. The developed color and its intensity seemed to depend on the stoichiometric ratio in which the plant extract and the metal ion had been mixed. Typical results are presented in Table 1.

### 2.4. Characterization of the synthesized gold nanoparticles

*UV–Visible spectroscopy:* The progress of GNP synthesis was monitored by recording the UV–Vis spectra in the wavelength range 190–1100 nm employing Labindia (model UV 3000) and ELICO (model SL 164) double beam UV–Visible spectrophotometers operated at 10 mm path length. The results are summarized in Table 1.

*SEM/TEM studies:* SEM (scanning electron microscopy) and TEM (transmission electron microscopy) studies were carried out to determine the size and morphology of the GNPs. To prepare for these studies the GNP-reactant mixtures were centrifuged at 12,000 rpm for 20 min using a Remi C 24 centrifuge. The resulting pellets were washed thrice with water to remove the unreacted constituents and were re-dispersed. The samples for SEM studies were prepared by placing a drop of this suspension on a carbon-coated SEM grid. For high resolution scanning electron microscopic studies the samples were prepared by placing dried pellets on a carbon coated aluminum stub. For TEM studies the samples were prepared by pelletizing the nanoparticles by diluting and through sonication. Each micrograph was recorded by depositing a drop of the well-dispersed samples on a carbon coated 300 mesh placed on copper TEM grid. Excess liquid was wiped off with a filter paper.

*Energy dispersive X-ray (EDAX) studies:* The elemental composition of the GNPs was assessed using the EDAX equipment attached to the SEM/HRSEM microscopes. The EDX spectrum was recorded after documenting the electron micrographs in the spot-profile mode by focusing on the densely occupied gold nanoparticle region.

*X-ray diffraction (XRD) studies:* An aliquot of the pelletized GNPs was drop-casted to a thin film on a glass slide and its X-ray diffraction spectra was recorded in the $2\theta$ region, from 0° to 80°, at a scanning rate of 0.02° per minute, and with a time constant of 2 s. The pattern of the crystallization of the GNPs was recorded using Cu $K_{\alpha 1}$ radiation with a wavelength ($\lambda$) of 1.5406 Å at a tube voltage of 40 kV and a tube current of 30 mA.

*Fourier transform infrared spectroscopic (FT-IR) studies:* For FT-IR spectroscopy, which was used to help in the identification of the functional groups involved in the reduction and stabilization of the gold nanoparticles, the samples were dried completely and ground with potassium bromide. The FT-IR spectrum was recorded at diffuse reflectance mode with 4 $cm^{-1}$ resolution in the mid-IR region between the wavenumbers 4000 and 400 $cm^{-1}$.

## 3. Results and discussion

### 3.1. UV–Visible spectra

On adding the plant extract to the gold (III) solution in select proportions (Table 1), gold nanoparticle formation commenced, with the gradual appearance of the characteristic yellow to pinkish red or violet GNP colors. These colors are known to appear due to the localized surface plasmon resonance (SPR) exhibited by the combined vibration of free conduction electrons of GNPs when induced by light (Mulvaney, 1996).

Single or double peaks occurred depending on the plant part used for preparing the extract and its concentration with respect to gold (III). With leaf extract only single peak was obtained while extracts of the stem and the roots gave two peaks each (Figs. 1–3). The second peak, when it occurred, was always in the NIR (near infra-red) region.

The presence of a single sharp SPR peak in the visible region is evidently due to the transverse (out-of-plane) plasmon resonance (TPR), which is exhibited by spherical nanoparticles. This was confirmed from the SEM and TEM studies, which showed that the particles synthesized using the leaf extract were indeed spherical in shape. On the other hand the presence of two prominent absorption bands – a low wavelength transverse absorption band in the visible region (out-of-plane vibration band) and a longer wavelength longitudinal absorption band in the NIR region (in-plane plasmon vibrations) – as in the root and stem extracts indicated that the synthesized particles possessed an intrinsic anisotropy (Link and El-Sayed, 2003; Shankar et al., 2005; Liz-Marzan, 2006). This was also confirmed by the SEM and TEM studies.

The results obtained from the UV–Visible spectral studies for all the reaction combinations are summarized in Table 1. It reveals that the optical density of the nanoparticles was found to increase gradually with an increase in the reaction duration, till it reached a maximum. It then either remained practically unchanged or began to decline.

The rate of reduction of gold ions present in the reaction medium was found to be almost complete within 6 h for the root extract and 24 h for the leaf and stem extracts (LE and SE) of the reaction duration.

#### 3.1.1. Electron microscopic (SEM, Hr-SEM, TEM and EDX) studies

The geometry of the synthesized GNPs was determined using SEM, Hr-SEM, and TEM techniques. The elemental composition of the nanoparticles was measured by EDX analysis.

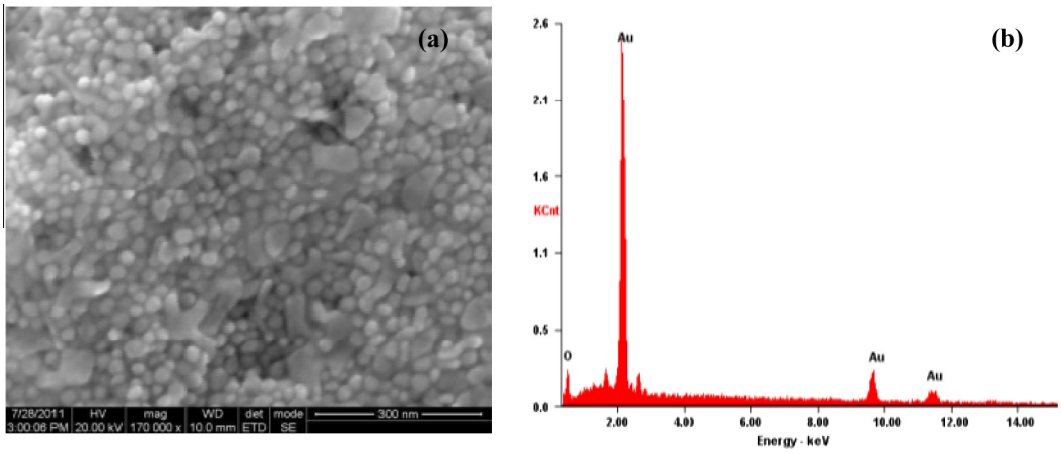


**Figure 4** The HR-SEM (a), and EDAX (b) image of GNPs formed with the leaf extract of ipomoea and gold (III).

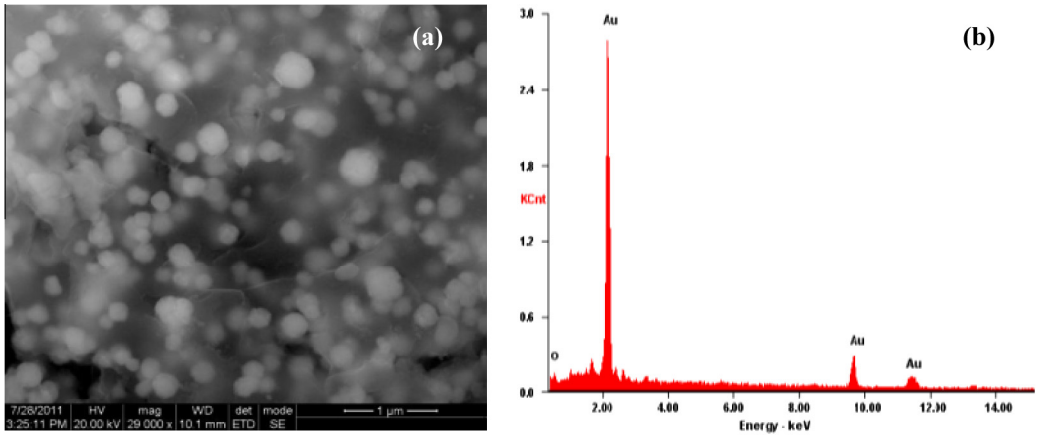


**Figure 5** The HR-SEM (a), and EDAX (b) image of GNPs formed with the steam extract of ipomoea and gold (III).

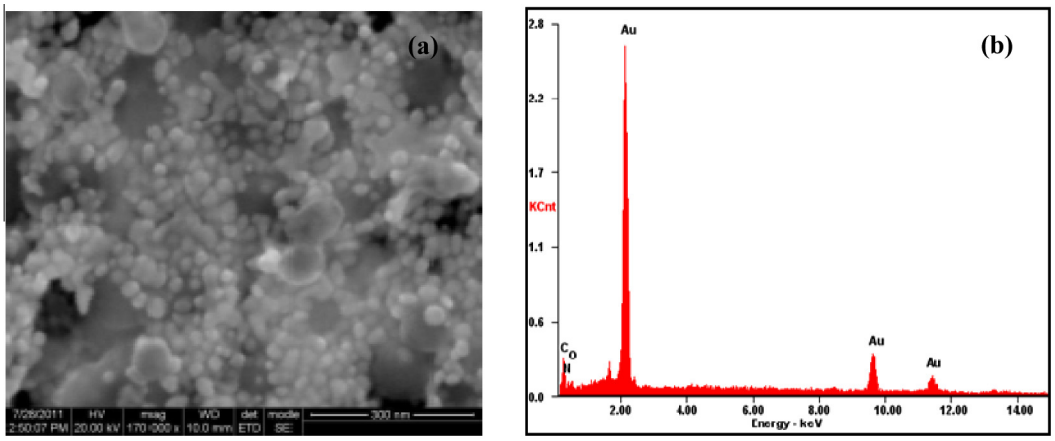


**Figure 6** The HR-SEM (a), and EDAX (b) image of GNPs formed with the root extract of ipomoea and gold (III).

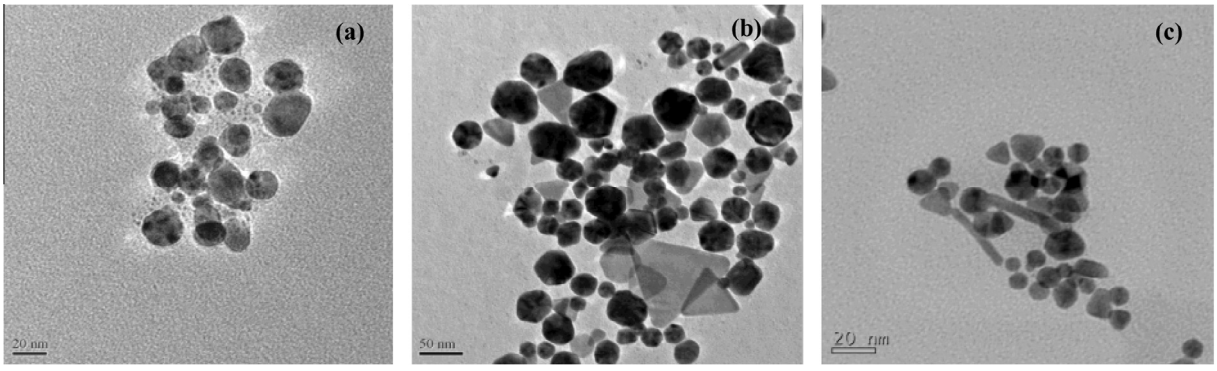


**Figure 7** Transmission electron micrographs of GNPs formed with the leaf extract (a), steam extract (b), and root extract (c) of ipomoea.

The SEM and Hr-SEM micrographs recorded for the GNPs synthesized with the Au (III) and leaf extract mixtures (Fig. 4) show that the nanoparticles are spherical in shape. The TEM micrographs for the GNPs arising from the same reactants reveal that the size of the NPs is in the range 3–40 nm (Fig. 7a).

The SEM, Hr-SEM and TEM images of the nanoparticles formed from the combinations of stem and root extracts with gold (III) are presented in Fig. 7(b and c). It is seen that these reaction combinations resulted in anisotropic nanoparticle formation with triangular, hexagonal, pentagonal, rod and truncated triangular shapes. The sizes of the nanoparticles were in the range 25–100 and 10–40 nm, respectively for the reactions involving the stem and the root extracts.

The EDX spectrum in the spot-profile mode shows a strong signal for gold (insets of Figs. 4–6). Weak signals from carbon, nitrogen and oxygen atoms are also seen which are likely to be due to X-ray emission from proteins/enzymes present in the

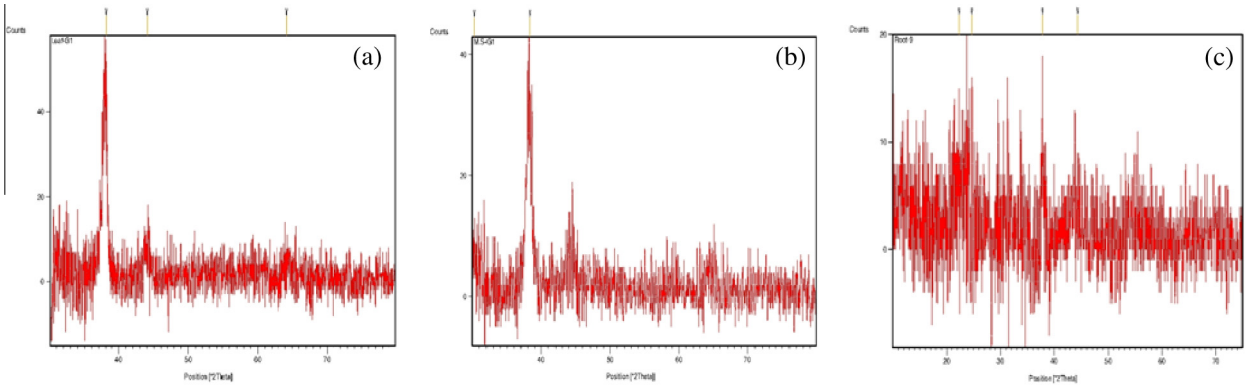


**Figure 8** X-ray diffraction spectrum of GNPs formed with the leaf extract (a), steam extract (b), and root extract (c) of ipomoea.

residual plant broths adhering to the GNPs. An optical absorption band at approximately 2 keV is seen, which is characteristic of gold nanoparticles (Anuradha et al., 2010, 2011b).

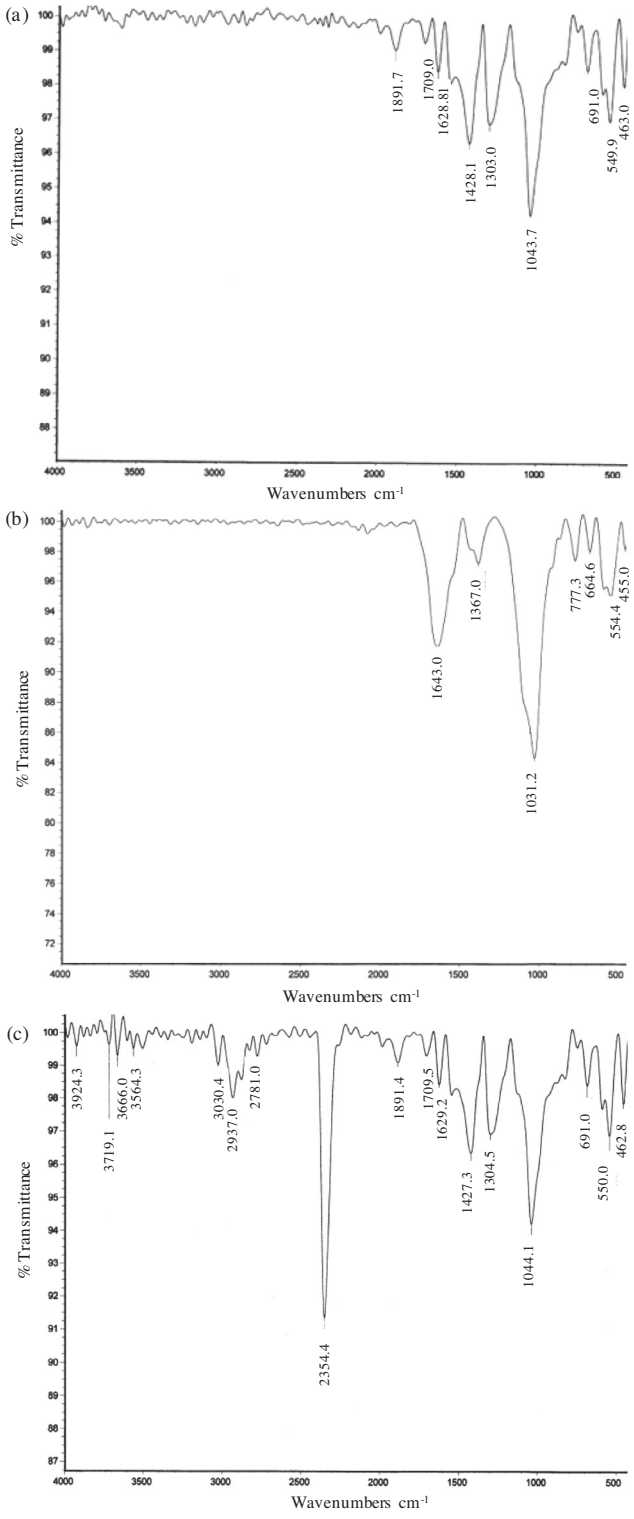


**Figure 9** The FTIR spectra of GNPs formed with the leaf extract (a), steam extract (b), and root extract (c) of ipomoea.

### *3.1.2. X-ray diffraction (XRD) studies*

The diffraction spectrum (Fig. 8) had intense peaks at 38.06, 38.28 and 37.80 $2\theta$ positions for GNPs formed with AU (III) and the leaf, the stem, and the root extracts, respectively. All correspond to (1 1 1) Bragg's planes and indicated a face-centered cubic structure (Shankar et al., 2003). From the XRD patterns which match with the database of JCPDS file No. 04-0784, it was established that the synthesized GNPs are of pure crystalline nature. The widening of Bragg's peak confirms the nanoparticle formation. The ratio of optical density between the (2 0 0) and (1 1 1) Bragg's diffraction peaks is 0.16. This is much lesser than the intensity ratio (i.e. 0.52) of conventional bulk gold, indicating that nanoparticles with (1 1 1) facets had been formed (Kareru et al., 2010).

### *3.1.3. Fourier transform infra-red (FT-IR) spectroscopy*

FT–IR spectral records were used to identify the functional group of biomolecules found in the plant broth which could have been involved in the nanoparticle synthesis. The FT-IR spectrum (Fig. 9) indicates that proteins and polysaccharides were possibly involved in the bioreduction and capping/stabilization of the synthesized GNPs.

The FT-IR pattern of leaf extract shows the presence of medium or strong absorption bands at 1428, 1303, and 1043 $cm^{-1}$. The strongest band (1043 $cm^{-1}$) can be assigned to C–N (amines) stretch (Elgersma et al., 2009; Kumar et al., 2010). The band at 1428 $cm^{-1}$ corresponds to O—H bond (carboxylic acids). In addition, a peak at 1303 $cm^{-1}$ corresponds to C–N stretch (amines). This shows that proteins and polysaccharides present in the leaf extract could be responsible for the reduction of the gold ions as well as coating or capping them to ensure their stability.

The peaks in the spectra of nanoparticles obtained with the stem extract were found at 1643 and 1031 $cm^{-1}$. In this case, too, the strongest band can be assigned to C–N stretch typical of amines (a peak at 1031 $cm^{-1}$) (Elgersma et al., 2009; Kumar et al., 2010). The band at 1643 $cm^{-1}$ corresponds to C═O stretch characteristic of amides (Kareru et al., 2010). Evidently, the proteins found in the stem extract have participated in the bioreduction and capping/stabilization of the synthesized GNPs.

The spectra of the root extract had bands at 1427, 1304 and 1044 $cm^{-1}$, corresponding to O–H bond (carboxylic acid), and C–N stretch (amines) of polysaccharides and proteins respectively (Kareru et al., 2008; Elgersma et al., 2009; Kumar et al., 2010). Hence, it can be inferred that polysaccharides and proteins have possibly played a key role in the bioreduction and capping/stabilization of the GNPs formed with the root extract.

## 4. Conclusion

Successful synthesis of gold nanoparticles (GNPs) using the otherwise worthless weed ipomoea (*I. carnea*) has been accomplished. Extracts from all the parts of the plant – the leaf, stem and root – were able to reduce as well as stabilize GNPs. By using different plant parts and by varying their proportion with reference to the metal concentration, GNPs of diverse geometry could be synthesized encompassing isotropic spherical and anisotropic triangular, pentagonal, hexagonal, rod and truncated triangular shaped particles of different sizes. The

purity and the crystallinity of the synthesized GNPs were confirmed by EDX, XRD and SAED studies. The FT-IR and EDX spectral studies together suggest that biomolecules were involved in the reduction of gold ions into GNPs and their subsequent stabilization by forming a coating around them.

**Acknowledgments**

The authors thank the University Grants Commission, New Delhi, for their support in the form of a Major Research Project (to TA and SAA) and Moulana Azad National Fellowship (to SAG).

**References**

Abbasi, T., Chari, K.B., Abbasi, S.A., 2008. Oussudu lake, Pondicherry, India: a survey on socio-economic interferences. Indian Geographical J. 83 (2), 149–162.

Abbasi, T., Anuradha, J., Abbasi, S.A., (2014). Use of plants in biomimetic synthesis of gold nanoparticles, J. Nano Res., in press

Anuradha, J., Abbasi, T., Abbasi, S.A., 2010. 'Green' synthesis of gold nanoparticles with aqueous extracts of neem (*Azadirachta indica*). Res. J. Biotechnol. 5 (1), 75–79.

Anuradha, J., Abbasi, T., Abbasi, S.A., 2011a. Biomimetic synthesis of gold nanoparticles using Aloe vera. Int. J. Environ. Sci. Eng. Res. 2 (1), 01–05.

Anuradha, J., Abbasi, T., Abbasi, S.A., 2011b. Rapid and reproducible 'green' synthesis of silver nanoparticles of consistent shape and size using *Azadirachta indica*. Res. J. Biotechnol. 6, 69–70.

APHA (American Public Health Association), (2012). Standard methods of water and wastewater. 22nd ed. American Public Health Association, American Water Works Association and Water Environment Federation publication, Washington, DC, USA.

Begum, N.A., Mondal, S., Basu, S., Laskar, R.A., Mandal, D., 2009. Biogenic synthesis of Au and Ag nanoparticles using aqueous solutions of Black Tea leaf extracts. Colloids Surf., B 71, 113–118.

Chari, K.B., Richa, Sharma, Abbasi, S.A., 2005. In: Comprehensive Environmental Impact Assessment of Water Resources Projects, vol. 1. Discovery Publishing House, New Delhi, p. xvi + 580.

Dubey, S.P., Lahtinen, M., Särkkä, H., Sillanpää, M., 2010. Bioprospective of *Sorbus aucuparia* leaf extract in development of silver and gold nanocolloids. Colloids Surf., B 80, 26–33.

Dubey, S.P., Dwivedi, A.D.D., Lahtinen, M., Lee, C., Kwon, Y., Sillanpaa, M., 2013. Protocol for development of various plants leaves extract in single-pot synthesis of metal nanoparticles. Spectrochimica Acta, Part A 103, 134–142.

Elgersma, R.C., Dijk, V.M., Dechesne, A.C., Nostrum, V.C.F., Hennink, W.E., Rijikers, D.T., Liskamp, R.M., 2009. Microwave-assisted polymerization for the synthesis of Abeta(16–22) cyclic oligomers and their self-assembly into polymorphous aggregates. Org. Biomol. Chem. 7, 4517–4525.

Kareru, P.G., Keriko, J.M., Kenji, G.M., Thiongo, G.T., Gachanja, G.N., Mukiira, H.N., 2010. Antimicrobial activities of skincare preparations from plant extracts. Afr. J. Tradit. Complement. Altern. Med. 7, 214–218.

Kumar, V., Yadav, S.C., Yadav, S.K., 2010. *Syzygium cumini* leaf and seed extract mediated biosynthesis of silver nanoparticles and their characterization. J Chem. Technol. Biotechnol. 85, 1301–1309.

Link, S., El-Sayed, M.A., 2003. Optical properties and ultrafast dynamics of metallic nanocrystals. Annu. Rev. Phys. Chem. 54, 331–366.

Liz-Marzan, L.M., 2006. Tailoring surface plasmons through the morphology and assembly of metal nanoparticles. Langmuir 22 (1), 32–41.

Mulvaney, P., 1996. Surface plasmon spectroscopy of nanosized metal particles. Langmuir 12, 788–800.

Shanker, S.S., Ahamd, A., Parsricha, R., Sastry, M., 2003. Bioreduction of chloroauratic ions by geranium leaves and its endophytic fungus yields gold nanoparticles of different shapes. J. Mat. Chem. 13, 1822–1826.

Shanker, S.S., Rai, A., Ankamwar, B., Singh, A., Ahmad, A., Sastri, M., 2004a. Biological synthesis of gold nanoprisms. Nature Mat. 3, 482–488.

Shanker, S., Rai, A., Ahmad, A., Sastry, M., 2004b. Rapid synthesis of Au, Ag, and bimetallic Au core-Ag shell nanoparticles using neem (*Azadirachta indica*) leaf broth. J. Colloid and Interface Sci. 275, 496–502.

Shankar, S.S., Rai, A., Ahmad, A., Sastry, M., 2005. Controlling the optical properties of lemongrass extract synthesized gold nanotriangles and potential application in infrared-absorbing optical coatings. Chem. Mater. 17, 566–572.

Sheny, D.S., Mathew, J., Philip, D., 2011. Phytosynthesis of Au, Ag and Au-Ag bimetallic nanoparticles using aqueous extract and dried leaf of *Anacardium occidentale*. Spectrochimica Acta, Part A 79, 254–262.

Singh, A.K., Talat, M., Singh, D.P., Srivastava, O.N., 2010. Biosynthesis of gold and silver nanoparticles by natural precursor clove and their functionalization with amine group. J. Nanoparticle Res. 12, 1667–1675.

Tettey, C.O., Nagajyothi, P.C., Lee, S.E., Ocloo, A., Minh An, T.N., Sreekanth, T.V.M., Lee, K.D., 2012. Anti-melanoma, tyrosinase inhibitory and anti-microbial activities of gold nanoparticles synthesized from aqueous leaf extracts of *Teraxacum officinale*. Int. J. Cosmetic Sci. 34, 150–154.